LHC POTENTIAL FOR THE HIGGS BOSON DISCOVERY

R. Kinnunen[1]

Helsinki Institute of Physics, P.O. Box 64, University of Helsinki, 00014 Helsinki, Finland

The searches for the Higgs boson(s) of the Standard Model and its Minimal Supersymmetric extension with the CMS and ATLAS detectors at the LHC are discussed.

1   Introduction

The CERN LHC collider is expected to start functioning within the next few years allowing the direct search for Higgs bosons in the full mass range. In this report, the LHC potential for the Higgs boson discovery is discussed in the framework of the Standard Model (SM) and its Minimal Supersymmetric extension (MSSM). In the SM Higgs mechanism, the Higgs boson mass m_H is a free parameter bounded from below to $m_H > 114.4$ GeV/c^2 by the LEP measurements [1]. The fits to the electroweak data favour a light Higgs boson with a central value of m_H = 114^{+69}_{-45} GeV/c^2 and a 95% CL upper limit of 260 GeV/c^2 [2]. The MSSM contains five Higgs bosons: the lighter scalar h, the heavier scalar H, the pseudoscalar A and the two charged bosons $H^{\pm}$. The MSSM parameter space is in general presented as a function of the pseudoscalar mass m_A and the ratio $\tan\beta$ of the vacuum expectation values of the two Higgs doublets. In most of the LHC studies, the remaining SUSY parameters are fixed to the values used in the LEP studies [3]: $M_2 = 200$ GeV/c^2, $\mu = -200$ GeV/c^2, $M_{\tilde{g}} = 800$ GeV/c^2, $M_{\tilde{q},\tilde{\ell}} = 1$ TeV/c^2. For the no-stop-mixing scenario A_t is set to zero and for the maximal mixing scenario A_t is set to 2450 GeV/c^2. The LEP measurements yield lower bounds of 91.0 and 91.9 GeV/c^2 for the masses of the h and A bosons in the MSSM [4]. The excluded $\tan\beta$ regions are 0.5< $\tan\beta$ < 2.4 for the maximal m_h scenario and 0.7< $\tan\beta$ < 10.5 for the no-stop-mixing scenario [4].

At tree level the h(H) mass is bound to be below(above) the Z boson mass but the radiative corrections, proportional to m^4_{top}, bring the upper (lower) bound to a significantly larger value. The one loop and dominant two loop calculations, with the SUSY parameters listed above and with a top quark mass of 175 GeV/c^2, predict an upper bound of 127 GeV/c^2 with maximal stop quark mixing [5]. This upper bound increases to 132 GeV/c^2 with the recent value of the top quark mass (178.3 GeV/c^2) from the Tevatron [6]. This change in the top mass affects the LHC expectations mainly through the maximum value of m_h, with renewed interest in the small $\tan\beta$ region.

---

[1]E-mail address: ritva.kinnunen@cern.ch

This report summarizes the CMS and ATLAS searches for the SM and MSSM Higgs bosons. The Higgs boson production and decay are discussed in Section 2. The CMS and ATLAS detectors are briefly presented in Section 3. Sections 4 and 5 discuss and summarize the discovery potential for the SM and MSSM Higgs bosons. Specific SUSY searches are discussed in Section 6, measurements of Higgs boson properties in Section 7 and conclusions are given in Section 8.

2 Higgs boson production and decay

In the SM, the Higgs boson production is dominated by the gluon-gluon fusion, $gg \rightarrow H$, over the full mass range $100 \lesssim m_H \lesssim 1$ TeV/c^2. The cross section is about 10 pb around $m_H \sim 200$ GeV/c^2. The QCD corrections for the $gg \rightarrow H$ process are large, with a next-to-leading (NLO) k factor ranging from 1.5 to 1.8 [7]. In the CMS studies, k factors are used for the channels (signal and the corresponding backgrounds) dominated by the $gg \rightarrow H$ process, like the inclusive $H \rightarrow \gamma\gamma$ channel. The other production processes, $qq \rightarrow qqH$, $q\overline{q}' \rightarrow HW$, $q\overline{q} \rightarrow HZ$, $gg/q\overline{q} \rightarrow t\overline{t}H$ and $gg/q\overline{q} \rightarrow b\overline{b}H$ have cross sections lower by one order of magnitude or more but often give possibilities for more efficient background suppression than in the gluon-gluon fusion process.

In the MSSM, the lighter scalar h is SM-like for $m_A > m_h^{max}$ (decoupling region), with production cross sections and decay partial widths close to those of the SM Higgs boson. At large $\tan\beta$, the couplings of the heavy neutral Higgs bosons to the electroweak gauge bosons are strongly suppressed, while those to the down-type fermions are enhanced with $\tan\beta$. The production of the heavy neutral MSSM Higgs bosons H and A proceeds mainly through $gg \rightarrow H/A$ and $gg/q\overline{q} \rightarrow b\overline{b}H/A$. At large $\tan\beta$, the $b\overline{b}H/A$ associated production dominates and is about 90% of the total rate for $\tan\beta \gtrsim 10$ and $m_A \gtrsim 300$ GeV/c^2. If the charged Higgs bosons are light, $m_{H^\pm} < m_{top}$, they are produced in $t\overline{t}$ events through the $t \rightarrow H^\pm b$ decay. Heavier $(m_{H^\pm} \geq m_t)$ charged Higgs bosons are mainly produced in the $gg \rightarrow t\overline{b}H^\pm$ process. When the associated b jet is not detected, the $gb \rightarrow tH^\pm$ process with integration over the final state b quark can be used [8].

For the SM-like Higgs boson, the $H \rightarrow b\overline{b}$ decay channel dominates for Higgs boson masses below 130 GeV/c^2. The branching fraction for $H \rightarrow \gamma\gamma$ is only $\sim 1.5\times10^{-3}$ for $m_H \lesssim 150$ GeV/c^2. For larger m_H, the decays are dominated by the $H \rightarrow WW^*/WW$ and $H \rightarrow ZZ^*/ZZ$ channels.

For the heavy neutral MSSM Higgs boson H and A, the branching fraction to $\tau^+\tau^-$ is about 10% and that to $\mu^+\mu^-$ about 3×10^{-4}. At small $\tan\beta$, the branching fractions to gauginos, when kinematically allowed, dominate and suppress the branching fractions to SM particles. The branching fraction to $t\overline{t}$, however, reaches $\sim 70\%$ at large m_A. The thresholds for decays to gauginos are sensitive to the SUSY parameters, in particular to $|\mu|$ and M_2, through the gaugino masses. Light charged Higgs bosons ($m_{H^\pm} < m_{top}$) decay to $\tau\nu_\tau$ with an almost 100% branching fraction. For $m_{H^\pm} \gtrsim 200$ GeV/c^2 the $H^\pm \rightarrow tb$ decay dominates at large $\tan\beta$ while the $H^\pm \rightarrow \tau\nu_\tau$ branching fraction decreases and is about 10% for $m_{H^\pm} \gtrsim 400$ GeV/c^2. The decay branching fractions to gauginos can reach $\sim 10\%$ at large $\tan\beta$ and $\sim 30\%$ at small $\tan\beta$, with the SUSY parameters listed in the introduction.

3   CMS and ATLAS Detectors

Detailed descriptions of the CMS and ATLAS detectors can be found in Refs. [10-13]. In CMS, the calorimeters are located between the tracker and the superconducting coil. Other features of the CMS detector are a strong 4T axial magnetic field, a multilayer muon system in the return yoke and a scintillating crystal electromagnetic calorimeter. The tracker, placed closest to the beam pipe, is made of fine-grained micro-strip and pixel detectors. The electromagnetic calorimeter is composed of about 80000 $PbWO_4$ crystals, with a single crystal front face of $\Delta\eta \times \Delta\phi = 0.0174 \times 0.0174$, covering the rapidity range up to $|\eta| < 3$. The sampling hadron calorimeter extends up to $|\eta| = 3$, and consists of 4 mm thick plastic scintillator tiles inserted between brass absorber plates. The outer hadron calorimeter is located in the central region of the detector, $|\eta| < 1.305$, outside the solenoid in the barrel return yoke to measure the late shower development. To extend the hermeticity of the hadron calorimeter up to $|\eta| = 5.191$, a separate forward calorimeter is placed at a distance of 11 m from the interaction point. The muon system [11] contains four stations of muon chambers (up to $|\eta| < 2.4$) and consists of drift tubes in the barrel region, cathode strip chambers in the endcap regions and resistive plate chambers in both barrel and endcap chambers.

In the ATLAS detector, the inner tracking system is placed inside a solenoid providing a 2T axial magnetic field. The electromagnetic and hadron calorimeters are outside the solenoid. The inner tracking detector consists of straw drift tubes interleaved with transition radiators for pattern recognition and electron identification, and several layers of semiconductor strip and pixel detectors providing high-precision space points. The electromagnetic calorimeter is a lead-liquid Argon sampling calorimeter with fine granularity and sampling for shower pointing and π^0 rejection. The endcap hadron calorimeters are based on the same technology as the electromagnetic calorimeter, with copper absorber plates. The barrel hadron calorimeter is an iron-scintillator sampling calorimeter with longitudinal tile geometry. The muon measurements are performed with air-core-toroid muon spectrometers in the barrel and endcap regions. The detectors are monitored drift tubes and resistive plate chambers in the barrel region and cathode strip and thin cap chambers in the forward regions.

4   Searches for a SM-like scalar Higgs boson H

A light SM-like Higgs boson with $m_H \lesssim 150$ GeV/c^2 can be searched for in the $H \to \gamma\gamma$, $H \to b\bar{b}$, $H \to ZZ^*/WW^*$ and $H \to \tau^+\tau^-$, decay channels. In this mass range the small natural width, $\Gamma_H \ll 1$ GeV, can be exploited by optimizing the mass resolutions in the $H \to \gamma\gamma$, $H \to ZZ^* \to \ell^+\ell^-\ell'^+\ell'^-$ and $H \to \mu^+\mu^-$ channels. A good mass resolution is particularly important for the inclusive search of the $H \to \gamma\gamma$ channel as the irreducible background from direct $pp \to \gamma\gamma + X$ production is large. The reducible background from $pp \to \gamma + jet + X$ production with the jet fragmenting into a leading isolated π^0 can be reduced below the irreducible one [10]. A Higgs boson mass resolution (σ of the Gaussian fit) of 0.65 GeV/c^2 can be obtained with the CMS detector at low luminosity for $m_H = 100$ GeV/c^2. Better signal-to-background ratios but much lower signal rates are obtained when this decay channel is searched for in the associated production processes WH and $t\bar{t}H$ with an isolated lepton from $W \to \ell\nu_\ell$ and in the H+jet production with a large E_T hadronic jet [13, 14].

The four-lepton final state from H $\rightarrow$ ZZ*/ZZ $\rightarrow$ $\ell^+\ell^-\ell'^+\ell'^-$ has been shown to provide a Higgs boson signature over a wide range of masses from $\sim$ 130 GeV/c^2 to about $\sim$ 600 GeV/c^2 [13, 14]. Backgrounds from the ZZ*, $t\bar{t}$ and Zb$\bar{b}$ can be efficiently suppressed with lepton isolation, an upper bound on the lepton impact parameter significance and cuts on the di-lepton invariant masses. The Higgs boson mass resolution with the CMS detector is found to be $\lesssim$ 1 GeV/c^2 in the four-muon channel [11] and between 1.3 and 1.8 GeV/c^2 in the four-electron channel [10] for $130 \leq m_H \leq 170$ GeV/c^2.

Around $m_H \sim 170$ GeV/c^2, where the H $\rightarrow$ ZZ*/ZZ branching fraction is smallest, the H $\rightarrow$ WW*/WW $\rightarrow$ $\ell^+\ell'^-\nu_\ell\overline{\nu}'_\ell$ channel can be exploited [13, 14]. For $m_H \lesssim 200$ GeV/c^2, the backgrounds from the WW, $t\bar{t}$ and Wt and production can be suppressed by taking advantage of WW spin correlations, which turn into small $\ell^+\ell^-$ opening angles for the signal. Central-jet vetoing suppresses further the $t\bar{t}$ and Wt backgrounds. As the Higgs boson mass reconstruction is not possible in this channel, a 5% systematic uncertainty has been assumed for the background determination [14].

The Higgs boson production in the gauge boson fusion qq $\rightarrow$ qqH has been shown to be important for the Higgs boson searches at LHC, in particular in the regions outside the reach of the four-lepton channel for $m_H \lesssim 130$ GeV/c^2 and $m_H \gtrsim 500$ GeV/c^2 [15]. In this process the hadronic jets from the final state quarks are energetic and distributed in the forward regions while no hadronic jets are expected in the central region. Tagging the forward jets and imposing a veto on central jets suppresses efficiently the backgrounds from $t\bar{t}$, W$\bar{t}$ and the QCD production of Z,γ^*+jet, WW and ZZ and hadronic multi-jets. The H $\rightarrow$ $\gamma\gamma$, H $\rightarrow$ WW* and H $\rightarrow$ $\tau^+\tau^-$ decay channels have been investigated in this production mode for $m_H \lesssim 150$ GeV/c^2 [13, 16, 17]. For $m_H \gtrsim 300$ GeV/c^2 advantage has been taken from the final states containing leptons, jets and E$_T^{\rm miss}$ with large branching fractions in the H $\rightarrow$ WW and H $\rightarrow$ ZZ decay modes [13, 14]. In the H $\rightarrow$ WW* $\rightarrow$ $\ell^+\ell'^-\nu_\ell\overline{\nu}'_\ell$ channel the WW spin correlations have been used to further suppress the backgrounds and to reconstruct a transverse mass from the lepton pair and the E$_T^{\rm miss}$ with an endpoint at the Higgs boson mass. The qq $\rightarrow$ qqh production process can be exploited to search for the Higgs boson also in the invisible final states, which could originate from the h $\rightarrow$ $\chi_1^\circ\chi_1^\circ$ decays in the MSSM. A model-independent 95% CL upper limit of $\sim$ 15% can be obtained for the Higgs boson branching fraction to invisible final states with an integrated luminosity of 10 fb^{-1} [16].

Figures 1 and 2 show the statistical significance for the SM Higgs boson for 30 fb^{-1} in the mass range of $100 \leq m_H \leq 800$ GeV/c^2 (with CMS) and for $m_H \leq 200$ GeV/c^2 (with ATLAS). In the CMS analysis, the significance is shown with k factors for the signal and for the backgrounds in the inclusive H $\rightarrow$ $\gamma\gamma$ channel and for the H $\rightarrow$ ZZ*/ZZ $\rightarrow$ $\ell^+\ell^-\ell'^+\ell'^-$ and H $\rightarrow$ WW*/WW $\rightarrow$ $\ell^+\ell'^-\nu_\ell\overline{\nu}'_\ell$ channels.

5 Searches for the MSSM Higgs bosons

In the MSSM, the suppression of the Higgs boson couplings to gauge bosons implies different search strategies. At large tanβ, the coupling enhancement to down-type fermions can be exploited to search the H and A bosons in the H,A $\rightarrow$ $\mu^+\mu^-$ and H,A $\rightarrow$ $\tau^+\tau^-$ decay channels in the associated production gg $\rightarrow$ b$\overline{b}$H/A. In this production process, the tagging of the associated b jets suppresses efficiently the Z, γ^* and QCD multi-jet backgrounds. A hadronic jet rejection of
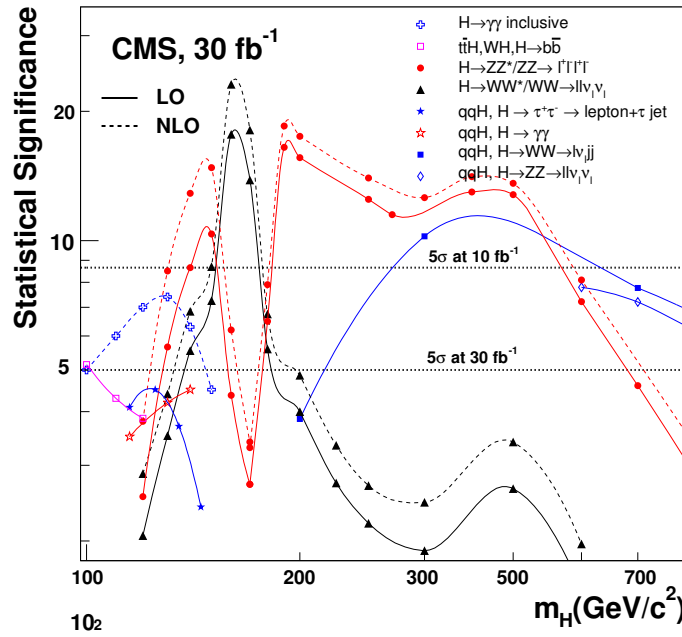
Fig. 1. Expected statistical significance for the SM Higgs boson as a function of m_H for 30 fb^{-1} with the CMS detector.

about 100 with an efficiency of about 50% for genuine b jets is expected with impact parameter measurement. In the $gg \rightarrow b\bar{b}H/A$ process, however, the overall b-jet finding efficiencies are lower due to the low E_T scale of the associated b jets. The $t\bar{t}$ and Wt backgrounds with genuine b's and τ's from the $W \rightarrow \tau\nu_\tau$ decays can be suppressed with a veto on an additional central jet.

For the H,A $\rightarrow \tau^+\tau^-$ decay channels, tagging of the τ's with impact parameter measurement can be used to further suppress the $Z \rightarrow \ell^+\ell^-$ and the QCD multi-jet backgrounds. To use the hadronic τ decays in the lepton-plus-τ-jet and two-τ-jet final states from the H,A $\rightarrow \tau^+\tau^-$ decay, an efficient hadronic τ trigger and τ-jet identification method is required to suppress QCD multi-jet and W+jet backgrounds with fake τ's from hadronic jets. A hadronic jet suppression of ~ 1000 has been shown to be possible with an efficiency of 20-30% for genuine τ jets, taking advantage of the narrowness and low multiplicity of the jets from hadronic τ decays [13]. The Higgs boson mass can be reconstructed in the H,A $\rightarrow \tau^+\tau^-$ channels from E_T^{miss} and the visible τ momenta exploiting the neutrino collinearity with the parent τ direction. The mass resolution improves for a decreasing opening angle between the two τ directions and is sensitive to the precision of the E_T^{miss} measurement. The eμ, two-lepton, lepton-plus-τ-jet and two-τ-jet final states have been studied for the H, A $\rightarrow \tau^+\tau^-$ decay modes [13, 14]. The mass resolution with the CMS detector at low luminosity is found to be $\sim 15\%$ for the two-τ jet final state, $\sim 20\%$ and for the lepton+τ jet final state and $\sim 25\%$ for the eμ or di-lepton final states, with $\Delta\phi_{\tau\tau} < 175°$.

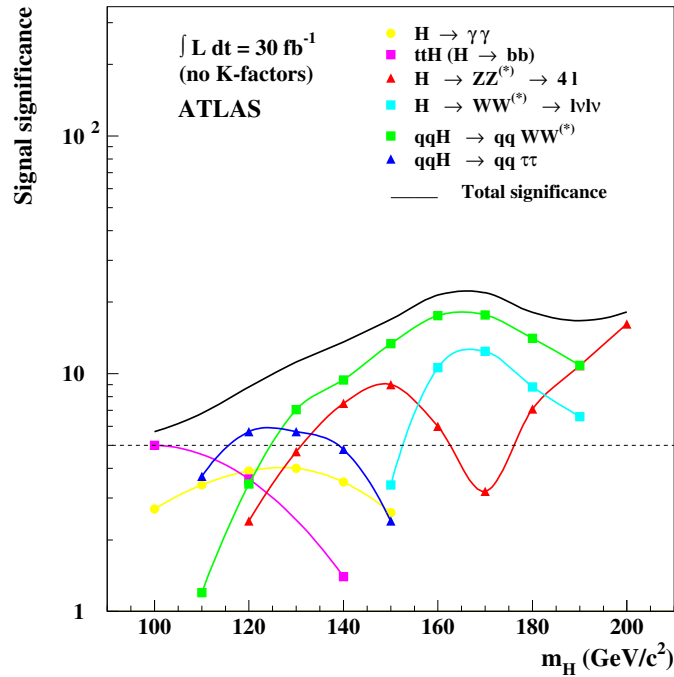For the $gg \rightarrow b\bar{b}H/A$, H/A $\rightarrow \mu^+\mu^-$ channel, the branching fraction is small but a good

Fig. 2. Expected statistical significance for the SM Higgs boson as a function of m_H for $m_H < 200$ GeV/c^2 for 30 fb^{-1} with the ATLAS detector.

mass resolution of $\sim 2\%$ can be obtained with the CMS detector. In the major part of the MSSM parameter space, this resolution is not enough to separate the signals from A and H, but may allow the measurement of the Higgs boson total width from the superposition of the A and H signals at large tanβ.

To search for the heavy charged Higgs bosons the $H^\pm \to \tau\nu_\tau$ decay channels with hadronic τ decays can be used in $t\bar{t}$ events in the region $m_{H^\pm} < m_{top}$, in the associated production process $gg \to btH^\pm$ for $m_{H^\pm} > m_{top}$ and also in the direct production $q\bar{q} \to H^\pm$ for $m_{H^\pm} > m_{top}$ [13, 14]. In these channels, the $t\bar{t}$ and Wt backgrounds with genuine τ's can be suppressed exploiting the different helicity correlations in the $H^\pm \to \tau\nu_\tau$ and the $W^\pm \to \tau\nu_\tau$ decays. Due to a more energetic leading pion from the $H^\pm$ decay a large background suppression can be obtained requiring at least 80% of the visible τ-jet energy to be carried by a single charged pion. For $m_{H^\pm} < m_{top}$, the $H^\pm$ signal is characterized by an excess of τ's in $t\bar{t}$ events relative to electrons and muons. For $m_{H^\pm} > m_{top}$, in the purely hadronic events with hadronic top decays, the E_T^{miss} originates mainly from the $H^\pm \to \tau\nu_\tau$ decay, making possible a reconstruction of the transverse mass from the τ jet and E_T^{miss} with an endpoint at $m_{H^\pm}$ for the signal and at m_W for the residual backgrounds.
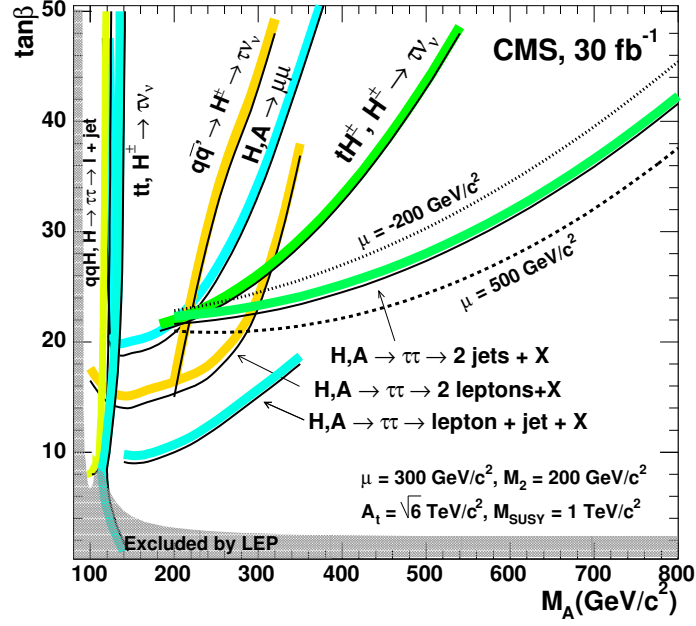
Fig. 3. The 5σ-discovery potential for the heavy MSSM Higgs bosons H, A and H$^\pm$ as a function of m_A and tanβ with maximal stop mixing for 30 fb^{-1} with the CMS detector.

Figure 3 shows the 5σ-discovery potential of CMS for the heavy neutral MSSM Higgs bosons H and A and for the charged Higgs bosons H$^\pm$ as a function of m_A and tanβ with maximal stop mixing for 30 fb^{-1}. The effect of the variation of the μ parameter on the discovery potential for the H $\rightarrow \tau^+\tau^- \rightarrow$ two τ-jet channel is also shown in Fig. 3.

Figure 4 shows the discovery potential for the lighter scalar MSSM Higgs boson h as a function of m_A and tanβ, assuming maximal stop mixing, $m_{top} = 175$ GeV/c^2 and $m_{SUSY} = 1$ TeV/c^2 for 30 fb^{-1}. The region of large m_A and tanβ is covered with h $\rightarrow \gamma\gamma$ in the inclusive production, h $\rightarrow$ b$\overline{\text{b}}$ in the associated production t$\overline{\text{t}}$h, h $\rightarrow$ ZZ$^* \rightarrow \ell^+\ell^-\ell'^+\ell'^-$ and h $\rightarrow \tau^+\tau^- \rightarrow \ell + \tau$ jet and h $\rightarrow \gamma\gamma$ in the gauge boson fusion qq $\rightarrow$ qqh. The region $m_A \gtrsim 400$ GeV/c^2 at large tanβ is not accessible with the h $\rightarrow$ b$\overline{\text{b}}$ and h $\rightarrow \tau^+\tau^-$ decay channels with an integrated luminosity as low as 30 fb^{-1} due to the decreasing branching fractions with increasing m_h. As the branching fraction for the h $\rightarrow$ ZZ* decay decreases fast with decreasing m_h, the discovery potential for the h $\rightarrow$ ZZ$^* \rightarrow \ell^+\ell^-\ell'^+\ell'^-$ channel is particularly sensitive to the MSSM parameters (mainly to the amount of stop mixing) and the top mass through the maximum value of m_h. With the recent value of the top quark mass, the discovery potential in this channel is expected to improve. The parameter space for $90 \lesssim m_A \lesssim 130$ GeV/c^2, where the lighter scalar is not SM-like, can be partly covered with the h $\rightarrow \mu^+\mu^-$ and h $\rightarrow \tau^+\tau^-$ decay channels with b tagging in the gg $\rightarrow$ b$\overline{\text{b}}$h production process [14].
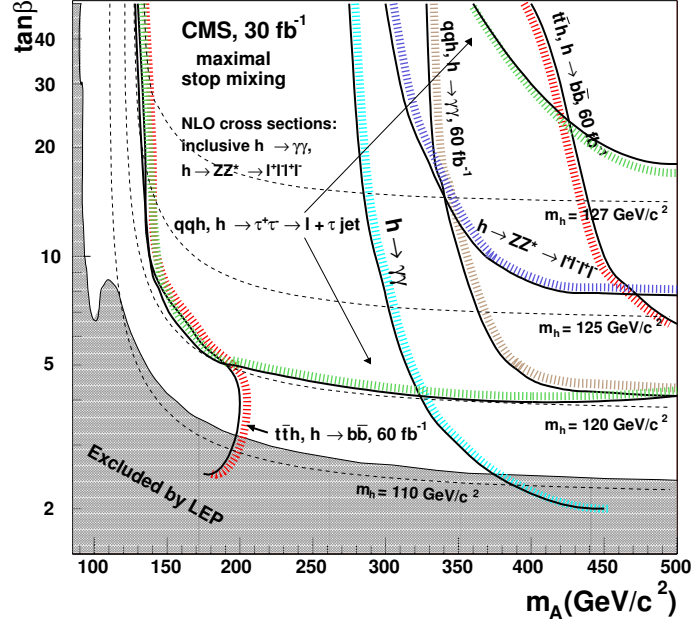
Fig. 4. The 5σ-discovery potential for the lighter scalar MSSM Higgs boson as a function of m_A and $\tan\beta$ with maximal stop mixing for 30 fb^{-1} with the CMS detector. The potential for the $t\bar{t}h$, $h \rightarrow b\bar{b}$ channel and for the $h \rightarrow \gamma\gamma$ channel in the $qq \rightarrow qqh$ process are shown for 60 fb^{-1}

6   Specific SUSY searches

The decays into SM particles may provide access to the heavy MSSM Higgs bosons only at large $\tan\beta$. The small and medium $\tan\beta$ values could be partly explored with Higgs boson decays to gauginos. If the gaugino masses are small enough, the branching fractions for the H, A $\rightarrow \chi_2^\circ \chi_2^\circ$ and H$^\pm \rightarrow \chi_{2,3}^\circ \chi_{1,2}^\pm$ decays can be sizeable. If the sleptons are also light ($m_{\tilde{\ell}} \lesssim$ 500 GeV/c^2) the branching fraction for the $\chi_2^\circ \rightarrow \tilde{\ell}\ell \rightarrow \chi_1^\circ \ell^+ \ell^-$ decay can be as large as $\sim$ 55% and four-lepton final states can be exploited. Figure 5 shows the 5σ-discovery region for the H, A $\rightarrow \chi_2^\circ \chi_2^\circ$ decay channel with the SUSY parameters fixed to M$_2$ = 120 GeV/c^2, $\mu = -$ 500 GeV/c^2, M$_{\tilde{q},\tilde{g}}$ = 1000 GeV/c^2 and M$_{\tilde{\ell}}$ = 250 GeV/c^2 for 30 and 100 fb^{-1}. The reduction of the discovery region with increasing M$_2$ is also shown.

In the MSSM, Higgs bosons can also be produced as decay products of gauginos in the squark and gluino cascades. More specifically, squarks and gluinos can decay to heavy charginos and neutralinos, $\chi_2^\pm$, χ_3° and χ_4°. If kinematically allowed, these particles decay into the lighter chargino and neutralinos, $\chi_1^\pm$, χ_1° and χ_2° and Higgs bosons. Squarks and gluinos can also decay directly to the light gauginos $\chi_1^\pm$ and χ_2° which then decay to the lightest neutralino and Higgs bosons. These events are characterized by large E$_T^{miss}$ and large jet multiplicity, which
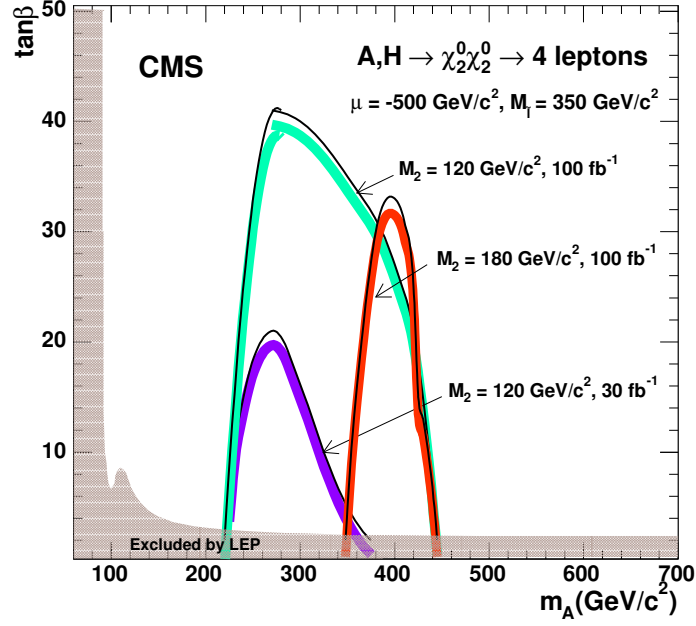
Fig. 5. The 5σ-discovery potential for the H, A $\to$ $\chi_2\chi_2 \to \ell^+\ell^-\ell'^+\ell'^-$ + X channel with $M_2 = 120$ and 180 GeV/c^2 for 30 and 100 fb^{-1}.

can be used to suppress efficiently the SM backgrounds The discovery potential with the $b\bar{b}$ decay channel has been shown to be for $m_A \lesssim 200$ GeV/c^2 and was found to be independent of $\tan\beta$ [18].

7   Measurements of Higgs boson properties

For the Higgs boson mass measurement, the best precision, about 0.1% for 300 fb^{-1}, is expected to be obtained with the H $\to \gamma\gamma$ and H $\to$ ZZ* $\to \ell^+\ell^-\ell'^+\ell'^-$ channels [14]. The precision of the mass measurement is limited with the uncertainty of the energy scale estimated to be 0.1% for muons, electrons and photons and 1% for hadronic measurements. The total decay width of the SM Higgs boson can be measured directly in the H $\to$ ZZ $\to \ell^+\ell^-\ell'^+\ell'^-$ channel for $m_H > 200$ GeV/c^2. The expected precision is about 10% for 300 fb^{-1} [14]. For $m_H < 200$ GeV/c^2, indirect methods (with a similar final precision) can be used with decay modes in the gluon-gluon fusion and weak gauge boson fusion production, assuming insignificant contributions from unknown decay modes [19]. The ratios of couplings and branching fractions have the advantage of partial cancellation of systematic uncertainties and can be measured with a precision better than 60% already with 30 fb^{-1} [20]. Measurements of Higgs boson spin and CP quantum numbers have been shown to be possible in the H $\to$ ZZ $\to \ell^+\ell^-\ell'^+\ell'^-$ channel
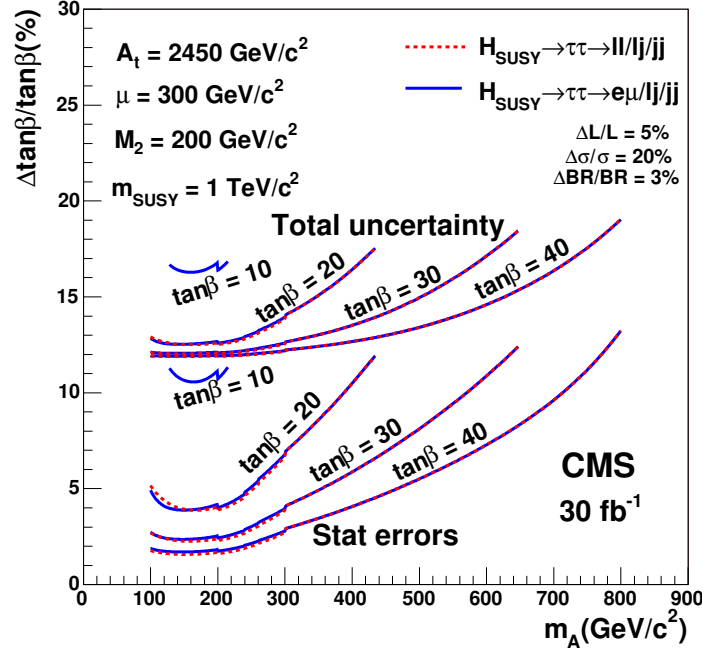
Fig. 6. Expected precision of the $\tan\beta$ measurement in the MSSM in the $H/A \to \tau\tau$ decay channels as a function of m_A for 30 fb^{-1} with CMS detector.

exploiting the helicity correlations in the decay angular distributions [21]. In the MSSM, the value of $\tan\beta$ can be measured from event rates in the $H, A \to \tau^+\tau^-$, $H, A \to \mu^+\mu^-$ and in $H^{\pm} \to \tau\nu_\tau$ decay modes exploiting the $\tan^2\beta$ dependence of the event rates at large $\tan\beta$. The uncertainty of the $\tan\beta$ measurement from the event rates in the $H, A \to \tau^+\tau^-$ channels is shown in Fig. 6 in the SUSY scenario given in Section 1 and assuming a 20% theoretical scale uncertainty and a 5% uncertainty in the luminosity measurement [22]. Uncertainty due to SUSY parameter measurement is not included.

8   Conclusions

The SM Higgs boson is expected to be found at the LHC with several decay channels over the full expected mass range in the CMS and ATLAS detectors. In the region 130 GeV/$c^2 \lesssim m_H \lesssim$ 500 GeV/c^2 the discovery is possible already with an integrated luminosity of 10 fb^{-1} or less with the $H \to WW^*/WW$ and $H \to ZZ^*/ZZ$ decay channels. The light SM Higgs boson with $m_H \lesssim 150$ GeV/c^2 is expected to be found in the inclusive $h \to \gamma\gamma$ channel, in the $h \to b\bar{b}$ decay in the associated $t\bar{t}H$ production and the weak boson fusion channels with decays to $H \to \gamma\gamma$, $H \to WW^*$ and $h \to \tau^+\tau^-$.

In the MSSM, the lighter scalar Higgs boson is expected to be found at large m_A and $\tan\beta$ with the inclusive $h \to \gamma\gamma$ and $h \to ZZ^* \to \ell^+\ell^-\ell'^+\ell'^-$ channels, with the $h \to \tau^+\tau^-$ channel in the gauge boson fusion $qq \to qqh$ already with 30 fb^{-1} and with the $h \to b\bar{b}$ decay channel in the associated production $t\bar{t}h$ with 60 fb^{-1}. The heavy neutral MSSM Higgs bosons can be found through the $H, A \to \mu^+\mu^-$ and $H, A \to \tau^+\tau^-$ decays channels at large $\tan\beta$. The two-lepton and lepton-plus-τ-jet final states from the $H, A \to \tau^+\tau^-$ decays cover the domain $m_A \lesssim 300$ GeV/c^2 and $\tan\beta \gtrsim 10$ already with 30 fb^{-1}. The two-τ-jet final states extend the sensitivity up to $m_A \sim 800$ GeV/c^2 with $\tan\beta \gtrsim 35$. The heavy scalar H is accessible also in the $H \to \tau^+\tau^-$ channel in the gauge boson fusion for $m_A \lesssim 120$ GeV/c^2 with 30 fb^{-1}. For the searches of the charged Higgs bosons the $H^\pm \to \tau\nu_\tau$ decay channel with hadronic τ decays plays a crucial rule. For $m_{H^\pm} < m_{top}$ the reach is for $m_A \lesssim 140$ GeV/c^2 in the $t\bar{t}$ events. The heavy charged Higgs bosons can be found in the associated production $tH^\pm$ at large $\tan\beta$ ($\gtrsim$ 20-30) and in the $qq' \to H^\pm$ fusion in a small part of the parameter space at large $\tan\beta$.

Part of the parameter space left outside the reach with SM particles at intermediate and small $\tan\beta$ region can be covered with the Higgs boson decays to neutralinos in the $H, A \to \chi_i^\circ \chi_j^\circ$ decay channel with the four-lepton final states. For the Higgs boson production from the gaugino decays in the $\tilde{g}, \tilde{q}$ cascades the region $m_A \lesssim 200$ GeV/c^2 is accessible already with 30 fb^{-1}, independent of $\tan\beta$.

References

[1] LEP Higgs Working Group: *Phys. Lett. B* **569** (2003) 61

[2] The LEP Electroweak Working Group, http://lepewwg.web.cern.ch/LEPEWWG/.

[3] M. Carena, S. Heynemeyer, C.E.M. Wagner, G. Weiglein, Suggestions for improved benchmark scenarios for Higgs-boson searches at LEP2, CERN-TH/99-374, DESY 99-186, hep-ph/9912223.

[4] LEP Higgs Working Group, Searches for the Neutral Higgs Bosons of the MSSM, hep-ex/0107030.

[5] S. Heinemeyer, G. Weiglein, Leading Electroweak Two-Loop Corrections to Precision Observables in the MSSM: *J. High Energy Phys.* **10** (2002) 072

[6] P. Azzi et al.,Combination of CDF and D0 Results on the Top-Quark Mass, hep-ex/0404010.

[7] R. Rainwater, M. Spira, D. Zeppenfeld, Higgs Boson Production at Hadron Colliders, hep-ph/0203187.

[8] T. Plehn, Charged Higgs Boson Production in Bottom-Gluon Fusion, hep-ph/0206121; E. Boos, T. Plehn, Higgs Boson Production Induced by Bottom Quarks, hep-ph/0304034.

[9] CMS Collaboration, Technical Design Reports: The Magnet Project CERN/LHCC 97-10, CMS TDR 1, 1997; The Tracker Project CERN/LHCC 98-6, CMS TDR 5, 199; The Hadron Calorimeter Project CERN/LHCC 97-31, CMS TDR 2, 1997; Trigger and Data Acquisition Systems CERN/LHCC 2000-38, CMS TDR 6.1, 2000; The Data Acquisition and High-Level Trigger Project CERN/LHCC 2002-26, CMS TDR 6.2, 2002

[10] CMS Collaboration, The Electromagnetic Calorimeter Project, Technical Design Report, CERN/LHCC 97-33, CMS TDR 4, 1997.

[11] CMS Collaboration, The Muon Project, Technical Design Report, CERN/LHCC 97-32, CMS TDR 3, 1997.

[12] ATLAS Collaboration, Technical Design Reports: Calorimeter Performance CERN/LHCC 96-40, 1997; High Level Trigger, Data Acquisition and Controls CERN/LHCC/2003-022; Inner Detector CERN/LHCC 97-16 and CERN/LHCC 97-17; Level 1 Trigger CERN/LHCC 98-14; Liquid Argon Calorimeter CERN/LHCC 96-41; Muon Spectrometer CERN/LHCC 97-22; Tile Calorimeter CERN/LHCC 96-42.

[13] A. Abdullin et al., Summary of the CMS Potential for the Higgs Boson Discovery, CMS NOTE 2003/033 and referencies therein.

[14] ATLAS Collaboration, ATLAS Detector and Physics Performance, Technical Design Report, ATLAS TDR 14, CERN/LHCC 99-14 and ATLAS TDR 15, CERN/LHCC 99-15.

[15] D. Zeppenfeld: *Int. J. Mod. Phys. A* **16** (2001) 831 T. Plehn, D. Rainwater, D. Zeppenfeld: *Phys. Rev. Lett.* **88** (2002) 051801

[16] G. Azuelos et al., Search for the SM Higgs boson using vector boson fusion at the LHC, Workshop on Physics at TeV Colliders, Les Houches, France, 2001, hep-ph/0203056.

[17] S. Asai et al., Prospects for the Search for a Standard Model Higgs Boson in ATLAS using Vector Boson Fusion: *Eur. Phys. J. C* **32** (2003) 209

[18] A. Datta, A. Djouadi, M. Guchait, F. Moortgat, Detection of MSSM Higgs bosons from SUSY particle cascade at the LHC, hep-ph/0303095.

[19] D. Zeppenfeld, R. Kinnunen, A. Nikitenko, E. Richter-Was, Measuring Higgs boson couplings at the LHC: *Phys. Rev. D* **62** (2000) 0130019/1-10

[20] M. Duhrssen, Prospects for the measurement of Higgs Boson coupling parameters in the mass range from 110 -190 GeV/c^2, ATLAS PHYS-2003-030.

[21] C.P. Buszello, I. Fleck, P. Marquard, J.J. vander Bij, Prospective Analysis of Spin- and CP-sensitive Variables in H $\to$ ZZ $\to \ell_1^+ \ell_1^- \ell_2^+ \ell_2^-$ with ATLAS, SN-ATLAS-2003-025.

[22] R. Kinnunen, S. Lehti, F. Moortgat, A. Nikitenko, M. Spira, Estimating the Precision of a tanβ Determination with H/A $\to \tau\tau$ and H$^\pm \to \tau\nu_\tau$ in CMS, Workshop on Physics at TeV Colliders, Les Houches, France, 2003, hep-ph/0406152.